Robust Spectral Denoising for Water-Fat Separation in Magnetic Resonance Imaging

Felix Lugauer[1,2], Dominik Nickel[3], Jens Wetzl[1], Stephan A.R. Kannengiesser[3], Andreas Maier[1,2], Joachim Hornegger[1]

[1] *Pattern Recognition Lab, Department of Computer Science, Friedrich-Alexander University Erlangen-Nuremberg, Erlangen, Germany*
[2] *Research Training Group 1773 "Heterogeneous Imaging Systems"*
[3] *MR Applications Predevelopment, Siemens Healthcare, Erlangen, Germany*

Introduction

Fat quantification using the multi-echo Dixon method is gaining clinical importance as it can match the accuracy of spectroscopy but provides high spatial resolution.

- **Non-invasive biomarkers from Dixon MRI[1]:**
  - Fat fraction (FF) – Diagnostics of hepatic steatosis, fibrosis, …
  - R_2^* relaxation – Indicator of liver iron concentration[2]
- **Strong noise bias in FF and R_2^* maps:**
  - Low SNR due to quant. protocol and breath-hold acquisition[3]
  - Noise amplification: biomarkers are estimated by fitting the low-SNR signal to a non-linear water-fat model[4] (*Fig. 1a*).

➔ **Enhance biomarkers by exploiting spectral redundancies between the series of contrast images with low SNR**

Methods and Experiments

- **Locally low-rank property**: signal model assumes two spectral components: water and fat (rank=2). Due to magnet imperfections, rank deficiency only for *locally correlated* voxels of contrast images (constant local magnetic field) (*Fig. 1b*).
- **Robust locally low-rank denoising (RLLR) using noise adaptive singular value thresholding (SVT):**

  1st pass: Data-driven noise estimation via median of normalized last singular value from local SVDs.

  2nd pass:

  a) Optimal thresholds based on noise $\hat{\sigma}_\epsilon$ and data (SURE[5]):

  $$\lambda_P = \mathrm{argmin}_\lambda \, \mathrm{SURE}(\mathcal{B}_P(\hat{\boldsymbol{X}}), \lambda, \hat{\sigma}_\epsilon^2)$$

  b) Sliding window SVT with averaging at overlaps (*Fig. 2).*

- In-vivo experiments on 3 volunteers with the following setup:

Scanner:	MAGNETOM Skyra @3T, 3-D gradient VIBE with PAT4 acceleration		
Flip angle:	2°	TR:	16.6 ms
FOV:	420 x 346 x 60 mm³	TEs:	1.06, 2.20, 3.69, 6.15, 9.84, 14.76 ms
Matrix:	160 x 132 x 60	Bandwith:	960 Hz/Px

Results and Discussion

- Evaluation of FF, R_2^* and model fit error without and with *RLLR.*

Qualitative:

➔ *structure-preserving noise removal, enhances detail (Fig. 2)*

Quantitative: avg. ROI measures for liver and spleen

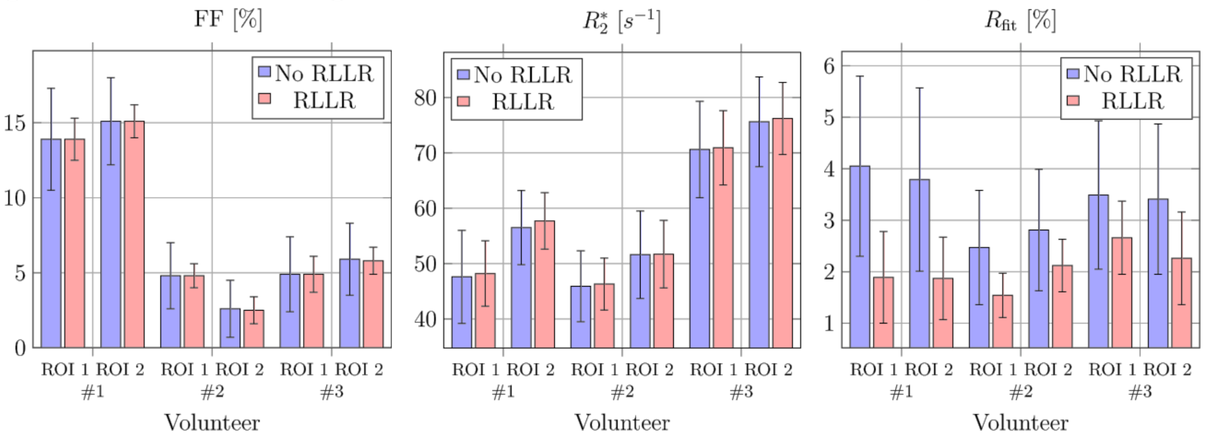

➔ *ROI mean is consistent while standard deviation (SD) drops.*

➔ *Denoising reduced model fit error by 37 % and eliminated uncertainty (SD) of fat fractions and R_2^* by 58 % and 24 %.*

Conclusions

- **RLLR** denoising is **automatic**, **robust** and **generically suited:**
  - No parameter tuning needed
  - Noise adaptive: no over- or under-regularization
  - For any spectrally sparse data: e.g., hyperspectral, dynamic
  - Structure-preserving noise bias removal

Contact
✉ felix.lugauer@fau.de
http://www5.cs.fau.de/~lugauer

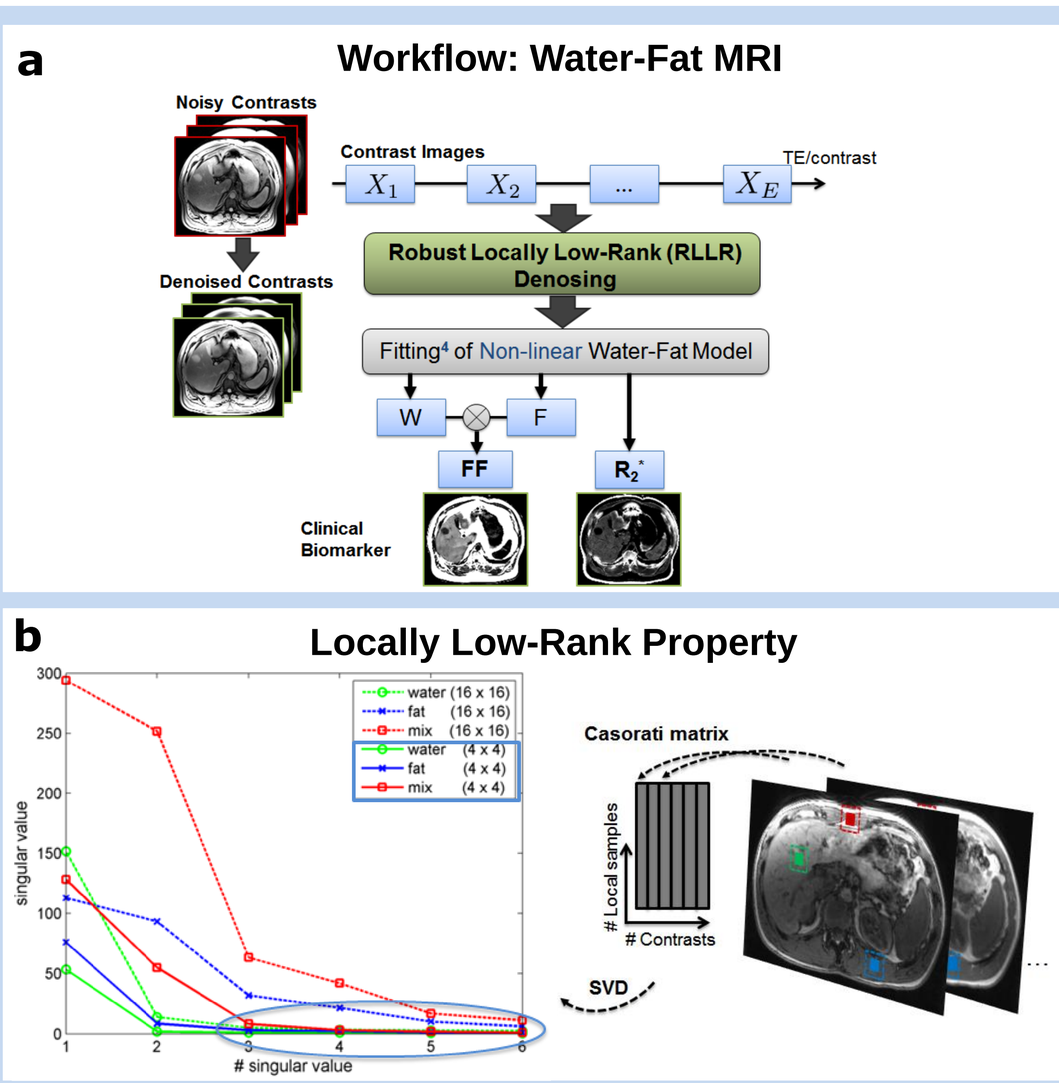

Fig.1: (a) Workflow for estimating biomarkers from contrast data (b) Low-rank property for sufficiently small patches

Signal model: $\boldsymbol{X}_e(j) = (\boldsymbol{W}(j) + c_e \boldsymbol{F}(j))\, \mathrm{e}^{i\boldsymbol{\Phi}(j,e)}, e \in [1,E], j \in [1,N]$

Block operator: $\mathcal{B}_P : \mathbb{C}^{N \times E} \to \mathbb{C}^{N_P \times E}, (E \ll N_P \ll N)$

Fat fraction: $\boldsymbol{FF}(j) = \dfrac{\boldsymbol{F}(j)}{\boldsymbol{W}(j) + \boldsymbol{F}(j)}$

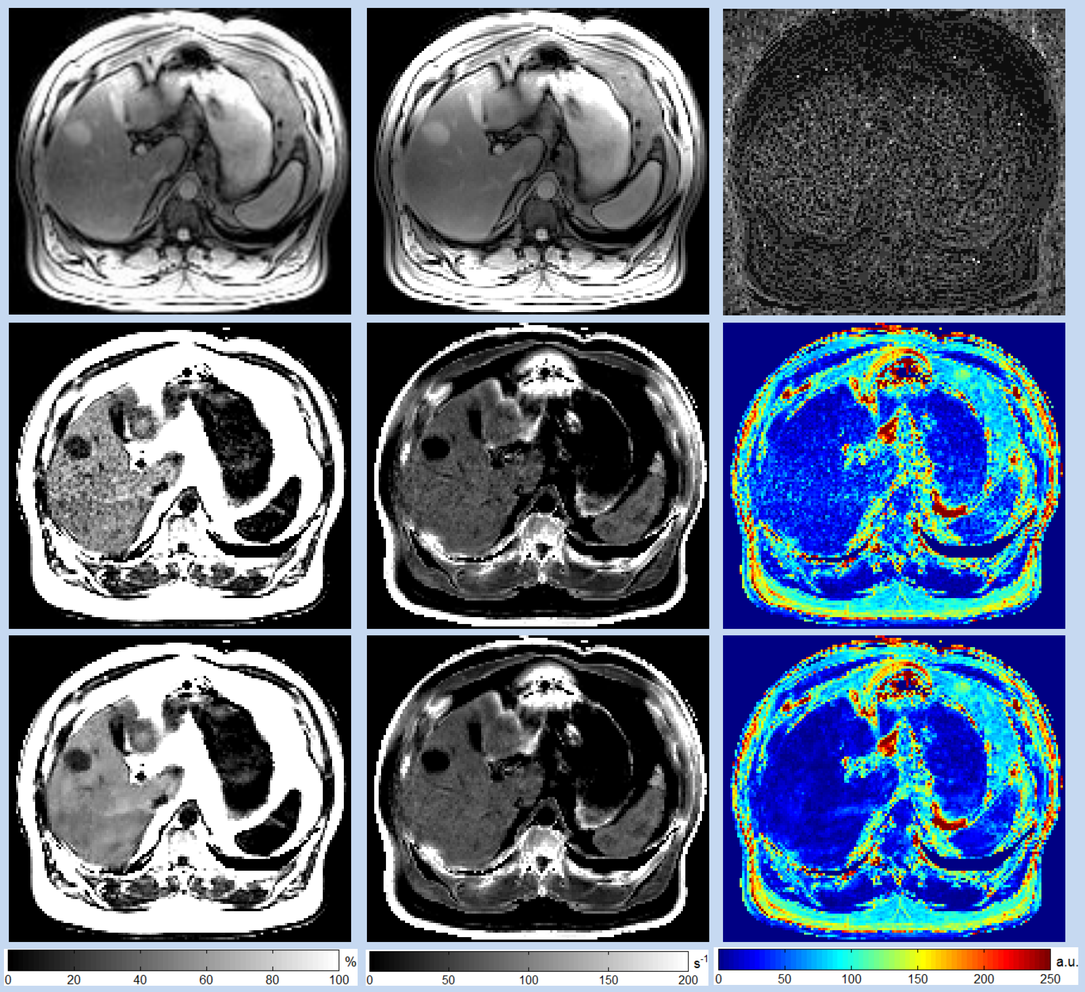

Fig.2: Row 1: Exemplary low-SNR contrast image. Original, denoised and their difference image (20x scaled) are shown from left to right. Noise bias was removed while details were enhanced, e.g., blood vessels in the liver. Row 2/3: Impact of denoising on the biomarker estimation: FF, R_2^* and associated fit error (left to right) using original and denoised data (bottom). Noise levels are lower in FF and R_2^* maps and the fit error is reduced for denoised data.

References

[1] Reeder, S. B. et al., JMRI, 34(4):729-749, (2011)
[2] Zhong, X. et al., MRM, 72(5):1353-1365, (2014)
[3] Liu, C.-Y. et al., MRM, 58(2):354-364, (2007)
[4] Candes, E. J. et al., IEEE Trans. Signal Process. 61:4643-4657, (2013)
[5] Sharma, P. et al., Diagn. Interv. Radiol., 20(1):17-26, (2014)

Acknowledgement: This work was supported by the Research Training Group 1773 *"Heterogeneous Image Systems",* funded by the German Research Foundation (DFG).